Skeletal Radiol (2001) 30:686–693
DOI 10.1007/s002560100399

ARTICLE

Konstantinos N. Malizos
Mihalis S. Siafakas
Dimitrios I. Fotiadis
Theofilos S. Karachalios
Panayotis N. Soucacos

An MRI-based semiautomated volumetric quantification of hip osteonecrosis

Received: 10 March 2000
Revision requested: 14 June 2000
Revision received: 1 May 2001
Accepted: 10 May 2001
Published online: 2 August 2001

K.N. Malizos (✉) · M.S. Siafakas
T.S. Karachalios
Department of Orthopaedics,
School of Health Sciences,
University of Thessalia, 22 Papakiriazi str.,
41222 Larissa, Greece
e-mail: kmalizos@otenet.gr
Tel.: +30-41-579191
Fax: +30-41-579190

D.I. Fotiadis
Department of Computer Science,
University of Ioannina, Ioannina,
45110 Greece

P.N. Soucacos
Department of Orthopaedic Surgery,
School of Medicine,
University of Ioannina, Ioannina,
45110 Greece

Abstract *Objective:* To objectively and precisely define the spatial distribution of osteonecrosis and to investigate the influence of various factors including etiology. *Design:* A volumetric method is presented to describe the size and spatial distribution of necrotic lesions of the femoral head, using MRI scans. The technique is based on the definition of an equivalent sphere model for the femoral head. *Patients:* The gender, age, number of hips involved, disease duration, pain intensity, limping disability and etiology were correlated with the distribution of the pathologic bone. Seventy-nine patients with 122 hips affected by osteonecrosis were evaluated. *Results:* The lesion size ranged from 7% to 73% of the sphere equivalent. The lateral octants presented considerable variability, ranging from wide lateral lesions extending beyond the lip of the acetabulum, to narrow medial lesions, leaving a lateral supporting pillar of intact bone. Patients with sickle cell disease and steroid administration presented the largest lesions. The extent of the posterior superior medial octant involvement correlated with the symptom intensity, a younger age and male gender. *Conclusion:* The methodology presented here has proven a reliable and straightforward imaging tool for precise assessment of necrotic lesions. It also enables us to target accurately the drilling and grafting procedures.

Keywords Osteonecrosis · Volumetric feature extraction · Automated diagnosis

Introduction

MRI is recognized as a sensitive tool with high specificity for the early recognition of osteonecrosis and is significantly more sensitive than radiographs or computed tomography [1, 2, 3, 4, 5]. A three-dimensional representation of the size, location and distribution of the necrotic lesion using MRI would allow for a more precise evaluation of the severity, prognosis, treatment selection and outcome evaluation [5, 6, 7, 8, 9, 10, 11].

Since the anatomic limits of the femoral head demonstrate significant variations in individuals, difficulties in expressing the percentage affected by avascular necrosis can be overcome by the introduction of the sphere equivalent concept. The sphere equivalent of the femoral head is defined as the sphere with the smallest radius enclosing the femoral head. The sphere equivalent of the femoral head, arbitrarily selected, has a larger volume than the corresponding anatomic femoral head and therefore the actual size of the lesion referred to the sphere equivalent of the femoral head can be expressed by a smaller percentile than that which refers to the anatomic femoral head. Previous classifications of small, medium and large lesions do not apply to this concept.

Table 1 Patient description according to etiology. Number of patients: *n*=79, number of hips: *n*=122 (right hip: 20, left hip: 16, bilateral: 43)

Etiology	Patient data				Hip data			
	Number	Male	Female	Mean age (years)	Number	Male	Female	Mean age (years)
Sickle cell disease	7	3	4	28	10	4	6	28
Corticosteroid	25	16	9	37	42	28	14	36.3
Alcohol	11	11	0	34	16	16	0	33.5
Injury	7	5	2	28.5	7	5	2	31
Immunosuppression	14	7	7	31.6	25	12	13	31
SLE	5	1	4	28.5	10	2	8	28
Idiopathic	10	6	4	31.6	12	8	4	29.8
Total	79	49	30		122	75	47	
Mean age (years)	32.8	33.4	31.8		32.4	33.2	31.2	
Age range (years)	17–54	17–54	17–52		17–54	17–54	17–52	

The purpose of this study was to introduce a more objective and precise methodology to describe the spatial distribution of osteonecrotic lesions, using digital image processing techniques and a reproducible concept to quantify data obtained from MRI films. The influence of various factors including etiology was also investigated.

Materials and methods

Osteonecrosis of the femoral head was evaluated in 79 patients of whom 49 were male and 30 were female with a mean age of 32.8 years. Preoperative MRI revealed 122 hips with oesteonecrosis. The disease was attributed to several etiologic factors, such as overuse of alcohol in 11 patients (16 hips), previous temporary use of corticosteroids in 25 patients (42 hips), continuous immunosuppressive medication in 14 patients (25 hips), femoral neck fractures in 7 patients (7 hips) previously treated surgically, sickle cell disease in 7 patients (10 hips), and systemic lupus erythematosus and continuous immunosuppressive medication, including steroids, in 5 patients (10 hips). In 10 patients (12 hips affected) the osteonecrosis was characterized as idiopathic. There was no significant difference in the mean age of patients with different etiologies except for those patients with steroid-related necrosis, who presented at a relatively higher mean age. (Tables 1, 2).

T1- and T2-weighted images, taken in increments of at most 4 mm in coronal sections, were selected to reconstruct three-dimensional images of the hips using the method described below. All MRI images were digitized with a VIDAR VXR 12 scanner (Vidar Systems Corporation, Va., USA) (Fig. 1). All data were processed on a SUN Sparc5 workstation (Sun Microsystems, Calif., USA) using the ANALYZE image analysis software Version 7.5 (Mayo Foundation, Minn., USA). The affected region, defined as the region with an abnormal signal, was outlined for each MRI slice using the tracing tool of the ANALYZE software. The smallest circle that circumscribed the femoral head was then identified. If flattening of the articular surface was present, its normal contour before collapse was reconstituted for each MRI slice by using the smallest circle that circumscribed the unaffected part. Using the radial divider tool of the software, the circle was divided into four regions and the affected area on each region was measured (Fig. 1).

The central slice or the largest section was used to construct the sphere equivalent of the femoral head based on the area measurement. The volume of the sphere was then calculated in cubic millimeters using the data from each MRI slice. The radius of the circle could easily be detected as shown in Fig. 2a.

Table 2 Hip description according to stage

Stage	Hips	Male	Female
Pre-collapse	23	14	9
Crescent sign	31	16	15
Post-collapse	68	45	23
Total	122	75	47

The sphere equivalent was divided into eight parts (octants) with three planes (coronal, sagittal and transverse) which intersected at the center of the sphere (Figs. 2b, 3). The abbreviations below are used to describe each octant and will be used henceforth:

ASL	Anterior superior lateral	PSL	Posterior superior lateral
ASM	Anterior superior medial	PSM	Posterior superior medial
AIL	Anterior inferior lateral	PIL	Posterior inferior lateral
AIM	Anterior inferior medial	PIM	Posterior inferior medial
ASL	Anterior superior lateral	PSL	Posterior superior lateral
ASM	Anterior superior medial	PSM	Posterior superior medial
AIL	Anterior inferior lateral	PIL	Posterior inferior lateral
AIM	Anterior inferior medial	PIM	Posterior inferior medial

In Fig. 3, a reconstructed three-dimensional femoral head is shown, with the affected area stained darker.

In order to compute the volume affected, a simplified Simpson's rule was used to integrate in the direction of the *x*-axis. The total affected volume per octant was computed using the formula:

$$V_{total} = \sum_{n=1}^{N} A_n d_n \quad (1)$$

where n is the MRI slice, A_n is the affected area of the MRI slice and d_n is the distance of the nth slice from the previous one. The above process ignores slice thickness since the average affected surface has been taken into account [12] The affected percentage per octant was computed as:

$$\alpha = \frac{V_{total}}{\left(\frac{1}{6}\pi R^3\right)}. \quad (2)$$

The extent of the lesion was expressed as a percentage of the corresponding octants affected. Although it was possible to measure the absolute value of the volume of the lesion and the sphere equivalent because of the differences in the size of the femoral

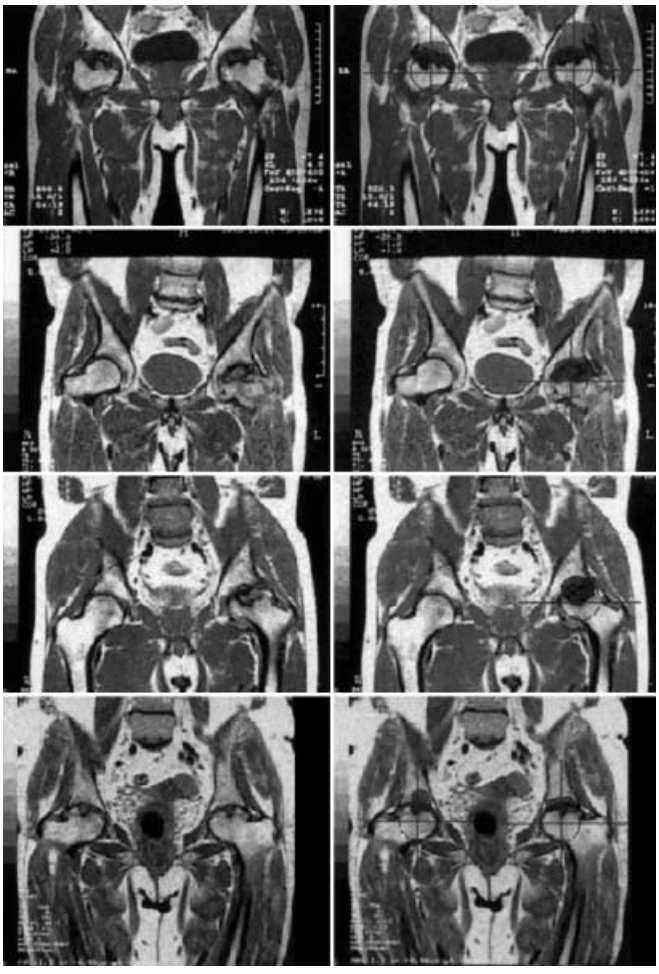

Fig. 1 Digitized (*left column*) and corresponding processed (*right column*) MRI images

heads among the individuals, it was more convenient to express the individual measurements as percentiles.

All measurements were carried out by three different assessors: an orthopaedic resident, an orthopaedic surgeon with experience in femoral head necrosis, and a radiologist with experience in MRI. The measurements were performed three times by each observer, with at least 1 week between readings. Intra-observer and inter-observer variability were assessed, setting 5 percentiles as the difference limit for agreement. There were five intra-observer differences in 122 measurements (95.9% intra-observer agreement) and 14 inter-observer differences in 122 measurements (88.5% inter-observer agreement). In those cases which showed differences in measurements, average percentile values were recorded and subsequently analyzed.

All measurements of the size of the lesion were expressed according to etiology, location of the affected segments and distri-

Fig. 3 Three-dimensional computerized reconstruction of the femoral head

Fig. 2 **A** Femoral head sphere equivalent. **B** Femoral head sphere representation and description with hemispheres and octants

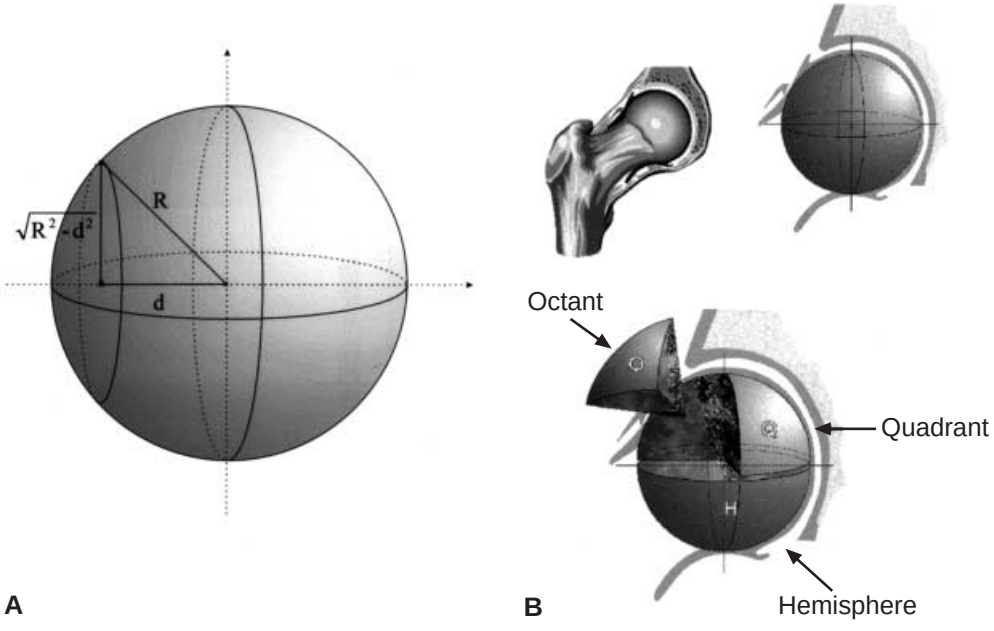

bution of the lesion in each octant. Statistical analysis of the various etiologic factors was performed using a one-way ANOVA, and post-hoc analysis was then performed using the LSD test. Comparison among segments was performed using the Students' *t*-test for dependent samples. Measures are expressed as mean± standard deviation (SD) unless otherwise indicated.

Validation study

We selected nine specimens of femoral heads obtained from elderly patients who had sustained femoral neck fractures and undergone hip hemi-arthroplasty. The specimens were trimmed and rounded up appropriately with the aid of wax, to take the shape of the sphere equal in diameter to the femoral head. In order to simulate the affected segment, part of the core of the femoral head was curetted out and then filled with a measured volume of surgical wax. MRI images at 4 mm increments were processed using the same technique as the index study.

The data obtained from the validation study demonstrated that the computerized measurements from the heads which were manually processed after hip hemi-arthroplasty operations were on average 5% larger (range 0.9–9%) than the measurements on the MRI images from the same specimens.

Results

Ninety-eight of the 122 affected hips were symptomatic at the time of their initial examination, and only 44% of the 43 patients with bilateral disease had symptoms in both hips. The time between the onset of hip pain and the MRI varied from 4 to 60 months (mean 19.27 months). The remaining 24 hips which were asymptomatic at the time of initial presentation were diagnosed by MRI.

Size of the lesion

The osteonecrotic segment of an equivalent to sphere femoral head ranged from 7% to 73% (mean 29%, SD ±16%). In patients with osteonecrosis associated with excessive use of alcohol or a history of surgically treated femoral neck fracture (FNF), the mean size of the necrotic part was 29% (±16%) and 29% (±15%) respectively. Femoral head involvement in patients who had previously been given corticosteroids temporarily and those who had received immunosuppressive medication continuously, averaged 32% (±18%) and 26% (±17%) respectively. In patients suffering from sickle cell disease it averaged 36% (±20%). Patients suffering from systemic lupus erythematosus (SLE) and those with idiopathic osteonecrosis presented an average size of lesion of 27% (±11%) and 23% (±12%) respectively (Table 3, Fig. 4).

When the one-way ANOVA test was used, no statistically significant differences in the size of the lesions amongst the different etiologies were found. However, the LSD test showed that patients with sickle cell disease have significantly larger lesions compared with those with idiopathic osteonecrosis (P=0.038).

Table 3 Percent of head volume affected (descending mean)

Etiology	Mean affected	Standard deviation	Range
Sickle cell disease	36	20	8–68
Corticosteroid	32	18	7–73
Alcohol	29	16	9–55
Injury	29	15	11–50
Immunosuppression	27	17	10–70
SLE	27	11	8–42
Idiopathic	23	12	9–40
% mean head affected	29	16	7–73

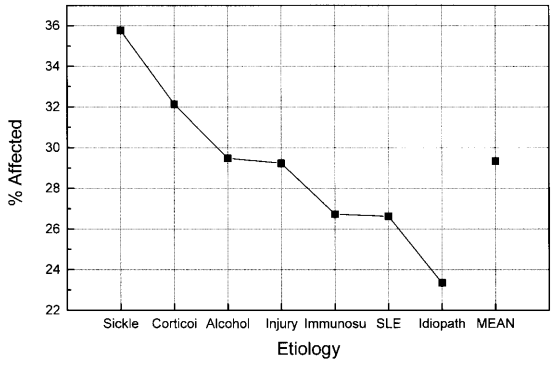

Fig. 4 Mean head volume affected by etiology (%). *MEAN* is the population mean

Distribution of the lesion

The ASM octant was the most extensively affected, the mean size of the necrotic segment being 59% (±28%) of the octant. The necrotic segment varied from 52% (±25%) in patients under immunosuppression to 71% (±31%) in patients with SLE-related necrosis. The PSM was the second most affected octant with a mean size of necrotic segment of 55% (±28) (mean range by etiology: 48–60%), followed by the ASL octant with an overall mean of 41% (±26%) (mean range by etiology: 31%–50%). The PSL octant had a mean size of lesion of 33% (±25) (mean range by etiology: 24–39%) and the two anterior-posterior octants, AIM and PIM, had mean values of 20% (±26%) and 13% (±19%) respectively (mean range by etiology: 5–37% in the former and 2–31% in the latter). The mean values for the AIL and PIL octants were 11% (±19%) (mean range by etiology: 1–25%) and 7% (±16%) (mean range by etiology: 2–28%) respectively (Table 4, Fig. 5).

One-way ANOVA test for the affected bone in the superior octants failed to demonstrate any significant differences in the distribution of the lesions among the etiologies. The LSD test showed that the ASL octant is less affected in cases considered as idiopathic compared with those in which the necrosis is related to injury or overuse of alcohol (P<0.05). In addition, the four lower octants –

Table 4 Percent volume affected for each octant (descending mean)

Octants	Mean affected	Standard deviation	Range
Anterior superior medial	59	28	4–100
Posterior superior medial	55	28	8–100
Anterior superior lateral	41	26	1–100
Posterior superior lateral	33	25	2 to 100
Anterior inferior medial	20	26	0–90
Posterior inferior medial	13	19	0 to 79
Anterior inferior lateral	11	19	0–94
Posterior inferior lateral	7	16	0–98

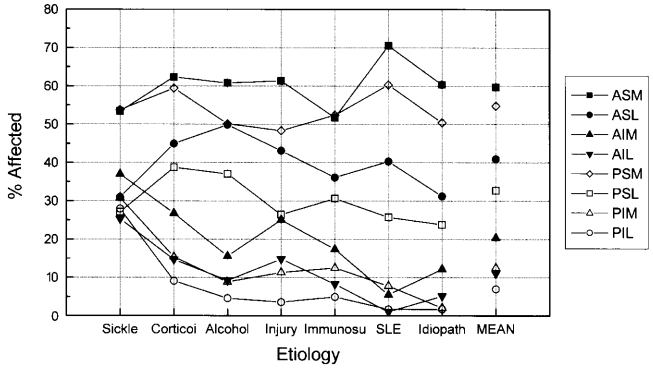

Fig. 5 Mean volume affected for each octant by etiology (%). *MEAN* is the octant population mean

AIM, AIL, PIM, PIL – were more affected in osteonecrosis related to sickle cell disease and corticosteroids (P=0.003–0.01).

Each octant of the superior half of the sphere equivalent, that is ASM, ASL, PSM and PSL, correlates with the other three in the following way, arranged in descending order of correlation coefficient: the highest with its neighbor on the coronal plane, then with its neighbor on the sagittal plane and the smallest with the octant located diagonally (r=0.2–0.74, P=0.00–0.05).

Although the cases investigated in this paper were carefully selected so that avascular necrosis could be attributed to only one etiologic factor, inevitably there was an overlap between patients suffering from SLE and those who had a history of corticosteroid and immunosuppressive medication. In order to examine whether this overlap had any effect on the results, we grouped all SLE, corticosteroid and immunosuppressive cases together and performed the statistical analysis again. There was no difference compared with the previous results.

Relation to other factors

Other factors taken into consideration were gender, age, number of hips involved, disease duration, pain intensity and limping disability. Only the symptomatic hips were taken into account when examining the femoral head measurements in relation to disease duration, pain intensity and limping disability. Below are cited all the statistically significant differences found in each of the abovementioned factors:

Table 5 Grouping by age, number of hips involved, disease duration, pain intensity and limping disability

	No. of hips in group	% PSM affected
Grouping by age		
Patients younger than 26 years	34	59
Patients 26–35 years	48	52
Patients older than 35 years	40	51
Grouping by number of hips involved		
Patients with only left hip involved	16	41
Patients with only right hip involved	20	64
Patients with both hips involved	86	53
Grouping by disease duration		
Patients with disease duration less than 12 months	53	45
Patients with disease duration 12–24 months	39	62
Patients with disease duration more than 24 months	30	62
Grouping by pain intensity		
Patients who did not report pain	24	18
Patients with slight pain	19	45
Patients with medium-intensity pain	50	60
Patients with severe pain	29	64
Grouping by limping disability		
Patients with no limping disability	28	38
Patients with slight limping disability	36	43
Patients with intermediate limping disability	40	64
Patients with severe limping disability	18	65

Gender

Male patients had a shorter disease duration (mean 16 months versus 24.6 months for females, P=0.02).

Age

Three groups were formed (Table 5) according to age. The anterior octants ASM, ASL, AIM and AIL were more affected in patients between 26 to 35 years of age than in the younger age groups (P=0.025–0.03).

Number of hips involved

Three groups were formed (Table 5) according to how many hips were affected. The PSM octant was more af-

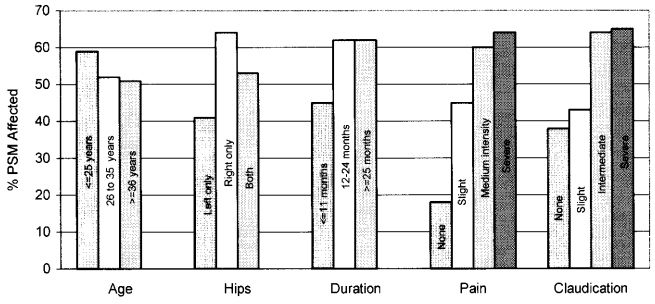

Fig. 6 Mean PSM volume affected by factors other than etiology (%)

fected in patients in whom only the right hip was involved than in those whose left hip only was affected (mean 64% versus 41%, P=0.027).

Disease duration

Three groups were formed (Table 5) according to the disease duration. ANOVA showed that there was a statistically significant difference in PSM octant involvement among all groups (P=0.04). It is less affected in patients with a disease duration of less than 12 months compared with those having a duration of 12–24 months (P=0.029) or more (P=0.04).

Pain intensity

Four groups were formed (Table 5) according to pain intensity. ANOVA showed that there was a statistically significant difference in PSM octant involvement among all groups (P=0.045). Specifically, the lesion was significantly smaller in patients with no pain than in those with moderate (P=0.045) or severe pain (P=0.035).

Limping disability

Four groups were formed (Table 5) according to the severity of limping disability. ANOVA showed that among all four groups there was a difference in the disease duration (P=0.029). Examining individual groups, patients with severe limping disability had a longer disease duration than those with slight (P=0.02) or intermediate (P=0.003) limping disability. In addition, the PSM octant was more affected in patients with intermediate limping disability than in those with slight limping disability (P=0.02).

The variation in PSM involvement with factors other than etiology is depicted in Fig. 6.

Discussion

A number of studies have indicated that the fate of osteonecrosis of the femoral head is affected by the extent, location and distribution of the necrotic lesion. Small lesions, away from the articular surface, have a more benign natural history if left untreated [1, 3, 13, 14]. In contrast, large lesions extending to the subchondral bone of weight-bearing regions demonstrate very rapid deterioration whether they are treated or not [1, 3, 8, 9, 14, 15, 16]. The need for a three-dimensional description of the lesion is thus justified. In this study, the actual size of each lesion was measured and expressed as a percentage of the sphere equivalent of the femoral head, thus normalizing size differences of femoral heads between patients.

The size of the lesion as measured by the methodology used in this study contradicts the measurements proposed by Steinberg et al. [14] and Koo et al. [3], who used calculations from central coronal MRI slices which were extrapolated from the total femoral head and not from three-dimensional reconstructed images. The integration of sequential slices at increments of 4 mm on which the affected segments with all their spatial irregularities were meticulously digitized, made possible the calculation of the actual affected volume. The affected segment collapse was adjusted by extraction of the area between the corresponding circle (for each slice) and the subchondral plate at its collapsed position. We also believe that these authors' measurements are less accurate because they account for the femoral head volume by using subjective limits of the femoral head [1, 2, 3, 4, 14, 17, 18, 19].

In the present study the pathologic bone was invariably located towards the medial, superior and anterior regions of the femoral head. In more advanced cases, collapse was also present in the same locations. These observations are consistent with biomechanically determined loading conditions at the corresponding articular surface. The resultant contact loads on the articular surface in the stance phase of the patient's gait are always directed inferiorly, laterally and posteriorly, from the acetabulum towards the femoral head [11, 20]. These directions do not change throughout daily activities regardless of the orientation of the hip. Most authors suggest that the various etiologic factors act through a common pathway, exerting an ischemic insult on a certain region of the femoral head [5, 20]. The uniform appearance of lesions in the superior, medial and anterior segments emphasizes the role of the mechanical environment under the articular surface of the femoral head as a major determinant of the location in which osteonecrosis is established. The various etiologic factors examined in our study did not appear to influence the location of the necrosis. Sickle cell disease, however, resulted in larger lesions than the other etiologic factors.

In contrast to the consistency of the location of the lesion in the femoral heads, there was a considerable variation in the size and distribution of the pathologic bone towards the superior-lateral octants. The extent of pathologic bone in the anterior-superior-lateral octant presented significant variability among the different etiologic factors, with alcohol and trauma being associated with significantly larger lesions. This observation emphasizes the prognostic value of an accurate assessment of the configuration and distribution of osteonecrosis, as wide lesions extending laterally beyond the lip of the acetabulum may be more susceptible to collapse compared with those contained medial to its limits. In narrow medially located lesions, a lateral supportive pillar of intact bone probably acts as a stress shield for the pathologic segment, protecting it from loads which may exceed its ultimate strength [19, 20]. As Steinberg et al. [14] and Koo and Kim [3] have demonstrated, apart from the stage and size of the lesion, the geographical distribution of the affected bone in relation to the weight-bearing surface determines, as a crucial factor, the prognosis and clinical outcome for any joint-preserving treatment for avascular necrosis [2, 3, 12, 14, 18, 19]. In an anatomically normal hip the articular surface of the femoral head measures 120% of the hemisphere, while the acetabulum is only 75% of the hemisphere. This means that the covered segment of the femoral head never exceeds 63% of its articular surface. Therefore broader lesions are barely contained in the acetabulum and become more susceptible to collapse [11].

ANOVA failed to show any statistically significant difference in the size and distribution of the lesion among the etiologies. This may be due to the fact that osteonecrosis is a chronic and evolving disease and therefore as the MRI scans were taken long after the symptoms started (range 4–60 months, mean 19.27 months) the contribution of mechanical factors would have superseded that of etiology, if any. Unfortunately there were only 24 hips without symptoms that could be tested for the potential effect of etiology on the size and distribution of the lesion – a number which was not adequate for statistical analysis, given the seven etiologies that were being considered.

The extent of PSM octant involvement correlates directly with the intensity of the symptoms, probably due to the exposure of the more affected area to continuous loading from contact forces. Also, the posterior octants are more affected at younger ages.

The accuracy and precision of the method employed in this study was validated in a laboratory setting on human specimens. The tendency to undersize the lesion by an average of 5% is probably related to the more ill-defined limits of the pathologic bone in some MRI images where the investigators preferred to trace the outermost limits of the pathologic signal [22]. This error is insignificant for all practical purposes, that is the severity, treatment selection and prognosis of the head osteonecrosis. A number of factors such as the quality of MRI imaging, the number and orientation of the available sections, image processing methodology, the presence of articular collapse and the use of appropriate image analysis hardware and software, may also influence the data. As the software becomes easier to use, the technique may provide a valuable tool for a more accurate assessment of size, location, configuration and distribution of necrotic lesions in the subchondral region of the femoral head. This may allow a more reliable prognosis and better selection criteria for treatment, as well as providing a means for evaluation of surgical results of the treatment. At present the method cannot be fully automated, since the physician must determine the sphere equivalent.

Other attempts at quantifying osteonecrosis have been reported. Koo and Kim [3] proposed measurement of angles on MRI slices. Both Steinberg et al.'s classification system [14] and the ARCO system recognize the importance of measuring the size of necrosis and scaling the severity of the disease. They propose the use of angles on either MRI or X-ray images for quantification of the femoral head in percentiles [14, 18, 20]. A major problem in these methods for quantification which use non-descriptive measurements in one plane is the lack of accuracy and low reproducibility in describing the three-dimensional configuration of the necrotic region based on one or two projections from radiographs or a central coronal MRI slice [23, 24, 25, 26]. In an extensive review of the imaging modalities for osteonecrosis we did not find an accurate descriptive tool for quantification which employs three-dimensional reconstruction from standard MRI sequence with multiple images. With the proposed method, the distribution and three-dimensional orientation of the pathologic bone in the subchondral area was precisely described.

In conclusion, the use of this method may offer a reasonable and straightforward imaging tool for quantification and volumetric description of osteonecrosis which is accurate for the size and the spatial configuration of lesions, provides a precise prognostic assessment, and may improve preoperative planning and intraoperative accuracy in cases of grafting procedures or drilling into the lesion. We are currently developing this method to make it simpler, easier to use and to expand its use to other skeletal sites where avascular necrosis occurs.

Acknowledgements I would like to thank Dr. A. Karantanas, MD Musculoskeletal Radiology specialist for his contribution in the Validation of our methodology. We thank Mrs. Aphrodite Katsaraki for her assistance in the statistical analysis of measurements. This work was partially supported by the donation of the image processing system by "Laikos Koumparas" to K.N.M.

References

1. Kerboul M, Thomine J, Postel M, Merle D'Aubigne R. The conservative surgical treatment of idiopathic aseptic necrosis of the femoral head. J Bone Joint Surg Br 1974; 56:291–296.
2. Koo KH, Kim R, Ko GH, Song HR, Jeong ST, Cho SH. Preventing collapse in early osteonecrosis of the femoral head: a randomized clinical trial of core decompression. J Bone Joint Surg Br 1995; 77:870–874.
3. Koo KH, Kim R. Quantifying the extent of osteonecrosis of the femoral head: a new method using MRI. J Bone Joint Surg Br 1995; 77:875–880.
4. Marcus ND, Enneking MD, Massam RA. The silent hip in idiopathic aseptic necrosis: treatment by bone-grafting. J Bone Joint Surg Am 1973; 55:1351–1366.
5. Sugano N, Takaoka K, Ohzono K, Matsui M, Masuhara K, Ono K. Prognostication of nontraumatic avascular necrosis of the femoral head. Clin Orthop 1993; 303:155–164.
6. Sakamoto M, Shimizu K, Iida S, Akita T, Moriya H, Nawata Y: Osteonecrosis of the femoral head: a prospective study with MRI. J Bone Joint Surg Br 1997; 79:213–219.
7. Mitchell DG, Rao VM, Dalinka MK et al. Femoral head avascular necrosis: correlation of MR imaging, radiographic staging, and clinical findings. Radiology 1987; 162:709–715.
8. Stulberg BN. Editorial comment of the fifth international symposium on bone circulation. Clin Orthop 1997; 334:2–5.
9. Bassounas A, Siafakas M, Fotiadis DI, Likas A, Malizos K. A quantitative method for the classification of osteonecrosis. Med Biol Eng Comput 1999; 37 [Suppl 2]:996–997.
10. Takatori Y, Kamogawa M, Kokudo T et al. Magnetic resonance imaging and histopathology in femoral head necrosis. Acta Orthop Scand 1987; 58:499–503.
11. Rab GT. Containment of the hip: a theoretical comparison of osteotomies. Clin Orthop 1981; 154:191–196.
12. Werahera PN, Miller GJ, Taylor GD, Brubaker T, Daneshgari F, Crawford ED. A 3-D reconstruction algorithm and extrapolation of planar cross sectional data. IEEE Trans Med Imaging 1995; 14;765–771.
13. Ohzono K, Saito M, Takaoka K et al. Natural history of nontraumatic avascular necrosis of the femoral head. J Bone Joint Surg Br 1991; 73:68–72.
14. Steinberg ME, Hayken GD, Steinberg DR. A quantitative system for staging avascular necrosis. J Bone Joint Surg Br 1995; 77:34–41.
15. Davison JJ, Coogan GP, Gunneson EE, Urbaniak RJ. The asymptomatic contralateral hip in osteonecrosis of the femoral head. In: Urbaniak JR, Jones JP Jr, eds. Osteonecrosis: etiology, diagnosis and treatment. American Orthopaedic Association, 1997:231–240.
16. Urbaniak JR, Coogan PG, Gunneson EB, Nunley JA. Treatment of osteonecrosis of the femoral head with free vascularized fibular grafting: a long-term follow-up study of one hundred and three hips. J Bone Joint Surg Am 1995; 77:681–694.
17. Ficat RP. Idiopathic bone necrosis of the femoral head. J Bone Joint Surg Br 1985; 67:3–9.
18. Steinberg ME, Bands RE, Parry S, Hoffman E, Chan T, Hartman KM. Does lesion size affect the outcome in avascular necrosis? Clin Orthop 1999; 366:262–271.
19. Herring JA, Neustadt, Williams JJ, Early JS, Browne RH. The lateral pillar classification of Legg-Calve-Perthes disease. J Pediatr Orthop 1992; 12:143–150.
20. Mont MA, Hungerford DS. Current concepts review: non-traumatic avascular necrosis of the femoral head. J Bone Joint Surg Am 1995; 77:459–474.
21. Lavernia CJ, Sierra RJ, Grieco FR. Osteonecrosis of the femoral head. J Am Acad Orthop Surg 1999; 7:250–261.
22. Jergesen HE, Heller M, Genant HK. Signal variability in magnetic resonance imaging of femoral head osteonecrosis. Clin Orthop 1990; 253:137–149.
23. Aaron K.R., Lennox D, Stulberg NB. The natural history of osteonecrosis of the femoral head and risk factors for rapid progression. In: Urbaniak JR, Jones JP Jr, eds. Osteonecrosis: etiology, diagnosis and treatment. American Orthopaedic Association, 1997:261–265.
24. Lafforgue P, Dahan E, Chagnaud C, Schiano A, Kasbarian M, Acquaviva PC. Early-stage avascular necrosis of the femoral head: MR imaging for prognosis in 31 cases with at least 2 years of follow-up. Radiology 1993; 187:199–204.
25. Beltran J, Knight CT, Zuelzer WA, et al. Core decompression for avascular necrosis of the femoral head: correlation between long-term results and preoperative MR staging. Radiology 1990; 175:533–536.
26. Kay RM, Lieberman JR, Dorey FJ, Seeger LL. Inter- and intraobserver variation in staging patients with proven avascular necrosis of the hip. Clin Orthop 1994; 307:124–129.